

# Short-Baseline Electron Neutrino Disappearance at a Neutrino Factory

CARLO GIUNTI<sup>a</sup>, MARCO LAVEDER<sup>b</sup>, AND WALTER WINTER<sup>c</sup>

<sup>a</sup> *INFN, Sezione di Torino, Via P. Giuria 1, I-10125 Torino, Italy*

<sup>b</sup> *Dipartimento di Fisica “G. Galilei”, Università di Padova and  
INFN, Sezione di Padova, Via F. Marzolo 8, I-35131 Padova, Italy*

<sup>c</sup> *Institut für Theoretische Physik und Astrophysik,  
Universität Würzburg, D-97074 Würzburg, Germany*

18 September 2009

## Abstract

We discuss short-baseline and very-short-baseline  $\nu_e$  disappearance at a neutrino factory. We take into account geometric effects, such as from averaging over the decay straights, and the uncertainties of the cross sections. We follow an approach similar to reactor experiments with two detectors: we use two sets of near detectors at different distances to cancel systematics. We demonstrate that such a setup is very robust with respect to systematics, and can have excellent sensitivities to the effective mixing angle and squared-mass splitting. In addition, we allow for CPT invariance violation, which can be tested (depending on the parameters) up to a 0.1% level.

---

<sup>a</sup>Email: giunti@to.infn.it

<sup>b</sup>Email: laveder@pd.infn.it

<sup>c</sup>Email: winter@physik.uni-wuerzburg.de

# 1 Introduction

Neutrino oscillation experiments have shown that neutrinos are massive particles with at least two squared-mass differences:  $\Delta m_{\text{SOL}}^2 \simeq 8 \times 10^{-5} \text{ eV}^2$ , measured in solar and very-long-baseline reactor neutrino experiments, and  $\Delta m_{\text{ATM}}^2 \simeq 2 \times 10^{-3} \text{ eV}^2$ , measured in atmospheric and long-baseline neutrino experiments (see Refs. [1–10]). These two  $\Delta m^2$ 's are perfectly accommodated in the framework of three-neutrino mixing, where there are two independent squared-mass differences. However, there are experimental anomalies which may indicate the existence of Short-BaseLine (SBL) or Very-Short-BaseLine (VSBL) oscillations generated by a third  $\Delta m^2$  which is much larger than the other two:  $\Delta m_{\text{SBL}}^2 \gtrsim 10^{-1} \text{ eV}^2$  or  $\Delta m_{\text{VSBL}}^2 \gtrsim 10 \text{ eV}^2$ . Among these anomalies, the most well-known is the LSND signal in favor of SBL  $\bar{\nu}_\mu \rightarrow \bar{\nu}_e$  oscillations [11], which has not been confirmed by other experiments and is currently disfavored by the negative results of KARMEN [12] and MiniBooNE [13]. Less well-known are the Gallium radioactive source experiments anomaly [14] and the Mini-BooNE low-energy anomaly [13], which could be explained by SBL [15, 16] or VSBL [17, 18]  $\nu_e$  disappearance.

The existence of a third  $\Delta m^2$  requires the existence of at least a fourth massive neutrino which corresponds, in the flavor basis, to the existence of a sterile neutrino  $\nu_s$ , *i.e.*, a fermion which is a singlet under the Standard Model symmetries. Hence it is electrically neutral and does not take part in weak interactions. If the three active neutrinos  $\nu_e$ ,  $\nu_\mu$ , and  $\nu_\tau$  are mixed with the sterile neutrino, neutrino oscillation experiments can observe the disappearance of active neutrinos into  $\nu_s$ .

In light of the above-mentioned anomalies, it is interesting to investigate the possibility of (V)SBL  $\nu_e$  disappearance with future high-precision experiments. In general, it is important to investigate the possibility of  $\nu_e$  disappearance generated by a  $\Delta m^2$  different from  $\Delta m_{\text{SOL}}^2$  and  $\Delta m_{\text{ATM}}^2$  in order to constrain schemes with mixing of four (see Refs. [1, 4, 6, 8]) or more [19, 20] massive neutrinos. These schemes have been studied mostly in connection with the LSND anomaly, but the latest global fits of the experimental data, including the LSND signal, are not good [4, 8]. However, the schemes with mixing of more than three neutrinos may be realized in nature independently of the LSND signal. Hence, it is important to investigate the phenomenology of sterile neutrinos with an open mind, not only through neutrino oscillations [21–29], but also by studying their effects in astrophysics [30–35] and cosmology [36–38].

If there is (V)SBL electron neutrino disappearance, it must be mainly into sterile neutrinos, because the mixing of the three active neutrinos with the fourth massive neutrino must be small in order to fit the data on  $\nu_e \rightarrow \nu_{\mu,\tau}$  oscillations generated by  $\Delta m_{\text{SOL}}^2$  and the data on  $\nu_\mu \rightarrow \nu_\tau$  oscillations generated by  $\Delta m_{\text{ATM}}^2$ . In the 3+1 four-neutrino schemes (see Refs. [1, 4, 6, 8]) with  $\Delta m_{(\text{V})\text{SBL}}^2 = |\Delta m_{41}^2| \gg \Delta m_{\text{ATM}}^2 = |\Delta m_{31}^2| \gg \Delta m_{\text{SOL}}^2 = |\Delta m_{21}^2|$ , where  $\Delta m_{kj}^2 \equiv m_k^2 - m_j^2$ , the mixing matrix  $U$  must be such that  $|U_{e4}|, |U_{\mu4}|, |U_{\tau4}| \ll 1$  and  $|U_{s4}| \simeq 1$ . Therefore, the amplitudes of the (V)SBL oscillation channels,  $A_{\alpha\beta} = 4|U_{\alpha4}|^2|U_{\beta4}|^2$  for  $\alpha \neq \beta$ , are such that  $A_{ab} \ll A_{as}$  for  $a, b = e, \mu, \tau$ .

In this paper we study the sensitivity of neutrino factory experiments to (V)SBL  $\nu_e$  and  $\bar{\nu}_e$  disappearance, which in practice has been investigated so far mainly through SBL reactor

neutrino experiments ( $\bar{\nu}_e$  disappearance).

We will first study, in Section 4, (V)SBL  $\nu_e$  and  $\bar{\nu}_e$  disappearance at a neutrino factory assuming exact CPT symmetry, which implies  $P_{ee} = P_{\bar{e}\bar{e}}$  (see Ref. [7]), considering the simplest case of effective two-neutrino mixing with

$$P_{ee} = P_{\bar{e}\bar{e}} = 1 - \sin^2(2\theta) \sin^2\left(\frac{\Delta m^2 L}{4E}\right), \quad (1)$$

where, from now on,  $\Delta m^2 = \Delta m_{(V)SBL}^2$ . This is the case of four-neutrino mixing schemes with  $\Delta m^2 = |\Delta m_{41}^2| \gg \Delta m_{ATM}^2 = |\Delta m_{31}^2| \gg \Delta m_{SOL}^2 = |\Delta m_{21}^2|$ . In the 3+1 schemes, the amplitude of the oscillations is related to the  $U_{e4}$  element of the mixing matrix by  $\sin^2(2\theta) = 4|U_{e4}|^2(1 - |U_{e4}|^2)$  (see Refs. [1, 4, 6, 8]).

The CPT symmetry is widely believed to be exact, because it is a fundamental symmetry of local relativistic Quantum Field Theory (see Ref. [39]). However, in recent years studies of extensions of the Standard Model have shown that it is possible to have violations of the Lorentz and CPT symmetries (see Refs. [40–42]) and several phenomenological studies of neutrino oscillations with different masses and mixing for neutrinos and antineutrinos appeared in the literature [43–54]. We will consider this scenario in the simplest case of effective two-neutrino mixing with

$$P_{ee} = 1 - \sin^2(2\theta_\nu) \sin^2\left(\frac{\Delta m_\nu^2 L}{4E}\right), \quad (2)$$

$$P_{\bar{e}\bar{e}} = 1 - \sin^2(2\theta_{\bar{\nu}}) \sin^2\left(\frac{\Delta m_{\bar{\nu}}^2 L}{4E}\right). \quad (3)$$

This kind of CPT violation in a four-neutrino mixing scheme could reconcile the LSND signal with the other neutrino oscillation data [50] and/or could explain the Gallium radioactive source experiments anomaly and the MiniBooNE low-energy anomaly together with the absence of  $\bar{\nu}_e$  disappearance in reactor neutrino experiments [18]. Let us emphasize that the reconciliation of the LSND anomaly with the results of other neutrino oscillation experiments is not possible in three-neutrino mixing schemes even if CPT violation is allowed [8, 52].

Another hint in favor of a possible CPT violation comes from the recent measurement of  $\nu_\mu$  and  $\bar{\nu}_\mu$  disappearance in the MINOS experiment [55], which indicate different best-fit values of the oscillation parameters of  $\nu_\mu$  and  $\bar{\nu}_\mu$ :  $\Delta\bar{m}_{MINOS}^2 \simeq 2 \times 10^{-2} \text{ eV}^2$  and  $\sin^2\bar{\theta}_{MINOS} \simeq 0.6$  for  $\bar{\nu}_\mu$ 's, whereas  $\Delta m_{MINOS}^2 \simeq 2.4 \times 10^{-3} \text{ eV}^2$  and  $\sin^2\theta_{MINOS} \simeq 1$  for  $\nu_\mu$ 's. The best-fit values and allowed region of the  $\nu_\mu$  oscillation parameters are in agreement with atmospheric  $\nu_\mu \rightarrow \nu_\tau$  oscillations. Since the 90% C.L. allowed region of the  $\bar{\nu}_\mu$  oscillation parameters has a marginal overlap with the much smaller 90% C.L. of the  $\nu_\mu$  oscillation parameters (see the figure in page 11 of Ref. [55]), the MINOS hint in favor of CPT violation is rather speculative. Nevertheless, it is interesting to notice that a global separate analysis of neutrino and antineutrino data in the framework of three-neutrino mixing with CPT violation leads to different best-fit values of the oscillation parameters of neutrinos and antineutrinos with  $\Delta\bar{m}_{ATM}^2 \simeq \Delta\bar{m}_{MINOS}^2$  and  $\sin^2\bar{\theta}_{ATM} \simeq \sin^2\bar{\theta}_{MINOS}$ , whereas  $\Delta m_{ATM}^2 \simeq \Delta m_{MINOS}^2$  and  $\sin^2\theta_{ATM} \simeq \sin^2\theta_{MINOS}$  [56]. However, in this paper we do not consider the MINOS hint in

favor of CPT violation. We concentrate our study on possible CPT violations in (V)SBL  $\nu_e$  and  $\bar{\nu}_e$  disappearance due to squared-mass differences larger than about  $0.1 \text{ eV}^2$ .

Besides those in Eqs. (2) and (3), it is possible to consider other, more complicated, expressions for  $P_{ee}$  and  $P_{\bar{e}\bar{e}}$ , with additional energy-dependent terms in the oscillation phases which could be generated by modified dispersion relations that are different for neutrinos and antineutrinos (see, for example, Refs. [57–62]). However, the introduction of more unknown parameters would make the analysis too cumbersome, without much additional information on the potentiality of a neutrino factory experiment to test CPT invariance. In fact, it is plausible that the additional energy-dependent terms in the oscillation phases generate spectral distortions which would make the identification of new physics even easier than in the simplest case that we consider.

In order to test CPT invariance (or *small* deviations from it) explicitly, it is convenient to define the averaged neutrino oscillation parameters

$$\theta \equiv \frac{1}{2}(\theta_\nu + \theta_{\bar{\nu}}), \quad \Delta m^2 \equiv \frac{1}{2}(\Delta m_\nu^2 + \Delta m_{\bar{\nu}}^2), \quad (4)$$

together with the CPT asymmetries

$$a_{\text{CPT}} \equiv \frac{\theta_\nu - \theta_{\bar{\nu}}}{\theta_\nu + \theta_{\bar{\nu}}}, \quad m_{\text{CPT}} \equiv \frac{\Delta m_\nu^2 - \Delta m_{\bar{\nu}}^2}{\Delta m_\nu^2 + \Delta m_{\bar{\nu}}^2}, \quad (5)$$

which are constrained in the range between  $-1$  and  $1$ . Then we have

$$\theta_\nu = (1 + a_{\text{CPT}})\theta, \quad (6)$$

$$\theta_{\bar{\nu}} = (1 - a_{\text{CPT}})\theta, \quad (7)$$

$$\Delta m_\nu^2 = (1 + m_{\text{CPT}})\Delta m^2, \quad (8)$$

$$\Delta m_{\bar{\nu}}^2 = (1 - m_{\text{CPT}})\Delta m^2. \quad (9)$$

The limit of CPT invariance (Eq. (1)) corresponds to  $a_{\text{CPT}} = m_{\text{CPT}} = 0$ . In Section 5 we discuss the potentiality of neutrino factory experiments to discover  $a_{\text{CPT}} \neq 0$  and/or  $m_{\text{CPT}} \neq 0$ .

The plan of the paper is: in Section 2 we define an “ideal detector” for the measurement of (V)SBL  $\nu_e$  and  $\bar{\nu}_e$  disappearance at a neutrino factory, and we describe our treatment of geometric effects; in Section 3 we discuss the requirements for systematics; in Section 4 we discuss the sensitivity to (V)SBL  $\nu_e$  and  $\bar{\nu}_e$  disappearance assuming CPT invariance, with the survival probability in Eq. (1); in Section 5 we discuss the sensitivity to CPT violation considering the survival probabilities in Eqs. (2) and (3); conclusions are presented in the final Section 6.

## 2 Ideal detector and geometric effects

Our neutrino factory geometry is based on the International Design Study for the Neutrino Factory (IDS-NF) baseline setup [63], with the geometry illustrated in Fig. 1. We consider

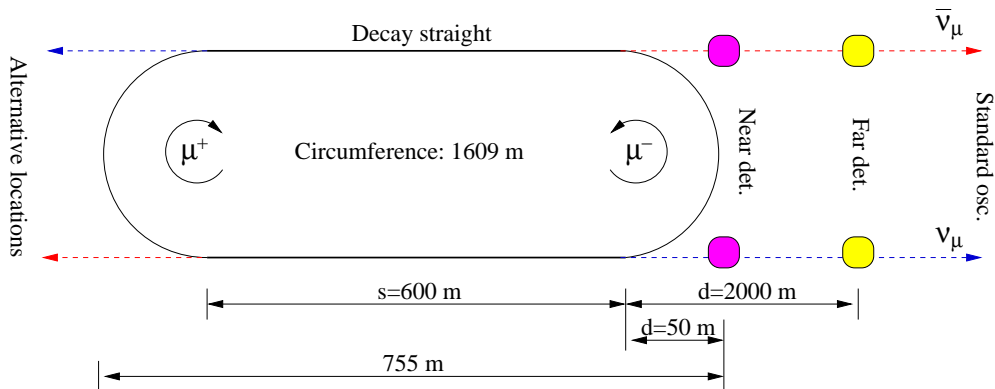


**Figure 1:** Geometry of the decay ring (not to scale). Two possible detector locations are shown at  $d = 50$  m and  $d = 2000$  m, where  $d$  is the distance to the end of the decay straight. The baseline  $L$  is the distance between production point and detector.

$2.5 \times 10^{20}$  useful muon decays per polarity and year, with muon energy  $E_\mu = 25$  GeV. For the total running time, we consider ten years.

In order to test SBL  $\nu_e$  disappearance, we add detectors in front of the decay straights as illustrated in Fig. 1. Here “near” and “far detectors” refer to SBL  $\nu_e$  disappearance only, whereas the detectors for standard oscillations are much farther away and not relevant for our problem. The straight sections are anticipated to be about  $s = 600$  m long. The distance  $d$  is the distance between the end of the decay straight and the near detector. The baseline  $L$  is the distance between production point and near detector, *i.e.*,  $d \leq L \leq d + s$ . Since the  $\mu^+$  and  $\mu^-$  are assumed to circulate in different directions in the ring, we need pairs of detectors in front of the straights because we want to test CPT invariance.<sup>1</sup>

Since there are no specifications for near detectors at a neutrino factory yet (see Ref. [64] for a generic discussion), we turn the argument around and formulate the requirements for the detectors for this measurement. Our detectors are assumed to measure the total charged current rates with a 100% detection efficiency; a lower efficiency will simply lead to a re-scaling of statistics and can be easily compensated by a larger detector mass. The energy threshold is chosen to be 500 MeV, similar to a Totally Active Scintillator Detector or an iron calorimeter, and the energy resolution is taken as

$$\Delta E = \varepsilon \sqrt{\frac{E}{E_0}}, \quad (10)$$

with  $\varepsilon = 0.55$  GeV and  $E_0 = 1$  GeV, which is a conservative estimate for a magnetized iron calorimeter [63]. Similarly, we assume that the neutral current level can be controlled at the level of  $10^{-3}$  from all neutrinos in the beam (see, *e.g.*, Refs. [65, 66] in the context of a low energy neutrino factory). However, we have tested that the results do not strongly depend on these three quantities. We require an excellent flavor identification (at the level of  $10^{-3}$  for the misidentification, as we will see later). Charge identification is also desirable in

<sup>1</sup>Without CPT invariance test, detectors in front of one straight are sufficient. The detectors in front of the other straight only increase statistics then.

order to reduce the contamination of the  $\nu_e$  (or  $\bar{\nu}_e$ ) signal by  $\bar{\nu}_e$  (or  $\nu_e$ ) generated by possible (V)SBL  $\bar{\nu}_\mu \rightarrow \bar{\nu}_e$  (or  $\nu_\mu \rightarrow \nu_e$ ) oscillations. However, we do not consider the backgrounds from charge misidentification explicitly.<sup>2</sup> For the binning, we use 17 bins between 0.5 and 25 GeV with a bin size of 0.5 GeV (1 bin) – 1 GeV (9 bins) – 2 GeV (5 bins) – 2.5 GeV (2 bins). As the main obstacles for the physics potential, we have identified the extension of the decay straights and the impact of systematics. We discuss the first issue below, and the second issue in the next section. Thereby, we define our “ideal detectors” as detectors with the above properties, but no backgrounds and systematics.

Our geometric treatment of the near detectors is based on Ref. [67], which discusses the flux at near detectors in detail. Here we start from the differential event rate from a point source  $dN_{\text{PS}}/dE$  without oscillations. Taking into account the extension of the straight and the geometry of the detector, the averaged differential event rate is given by<sup>3</sup>

$$\frac{dN_{\text{avg}}}{dE} = \frac{1}{s} \int_d^{d+s} \frac{dN}{dE} dL = \frac{1}{s} \int_d^{d+s} \frac{dN_{\text{PS}}(L, E)}{dE} \varepsilon(L, E) P_{ee}(L, E) dL. \quad (11)$$

Here  $\varepsilon(L, E) = A_{\text{eff}}/A_{\text{Det}}$  parameterizes the integration over the detector geometry for a fixed baseline  $L$  and given energy  $E$  ( $A_{\text{Det}}$  is the surface area of the detector and  $A_{\text{eff}}$  is the effective surface area which takes into account the angular dependence of the neutrino flux). Since  $dN_{\text{PS}}/dE \propto 1/L^2$ , we can re-write this as

$$\frac{dN_{\text{avg}}}{dE} = \frac{dN_{\text{PS}}(L_{\text{eff}}, E)}{dE} \frac{L_{\text{eff}}^2}{s} \int_d^{d+s} \frac{\varepsilon(L, E)}{L^2} P_{ee}(L, E) dL = \frac{dN_{\text{PS}}(L_{\text{eff}}, E)}{dE} \hat{P}(E), \quad (12)$$

with the average efficiency ratio times probability<sup>4</sup>

$$\hat{P}(E) \equiv \frac{L_{\text{eff}}^2}{s} \int_d^{d+s} \frac{\varepsilon(L, E)}{L^2} P_{ee}(L, E) dL, \quad (13)$$

and the effective baseline

$$L_{\text{eff}} = \sqrt{d(d+s)}, \quad (14)$$

such that  $\hat{P}(E) = 1$  for  $\varepsilon(L, E) \equiv P_{ee}(L, E) \equiv 1$ . We assume  $\varepsilon(L, E) \equiv 1$  (far distance approximation), which, to a good approximation, is satisfied for ND4 of Ref. [67] (see Fig. 4 therein) for  $d \gtrsim 50$  m. This detector is very small (200 kg), however, with a sufficient event rate. At a neutrino factory, the active volume of near detectors are probably going to be rather small, because high granularity and good track reconstruction will be more important

<sup>2</sup>The level of contamination depends on the oscillation model. Even for large mixing angles driving these oscillations of the potential background, a charge misidentification level of about  $10^{-3}$  would be sufficient.

<sup>3</sup>Note that as a peculiarity compared to Ref. [67],  $dN_{\text{PS}}/dE$  uses the unoscillated event rate, because the oscillation probability has to be integrated over.

<sup>4</sup>Note that Eq. (12) implies that in GLoBES a point source spectrum at the effective baseline  $L_{\text{eff}}$  can be used, which has to be corrected by Eq. (13). We perform Eq. (13) directly in the probability engine.

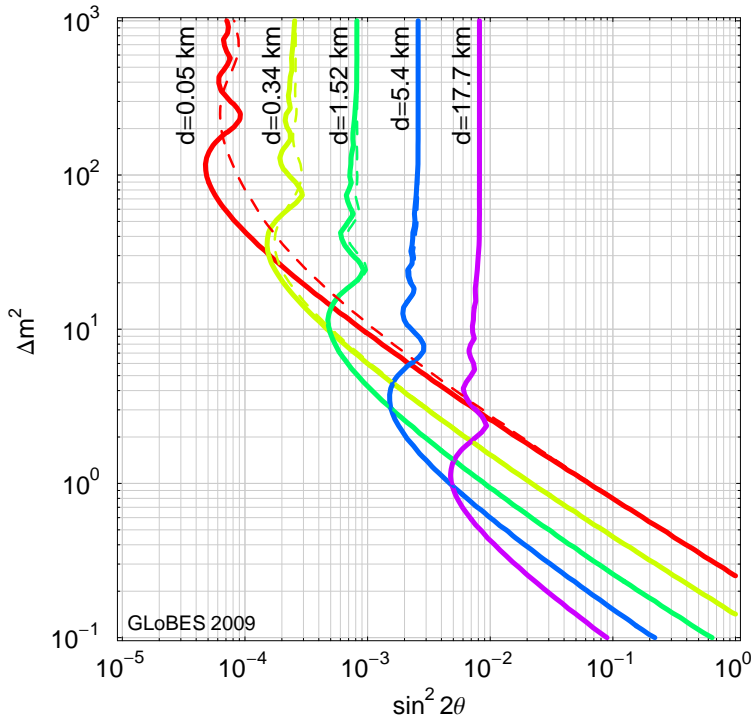


**Figure 2:** Exclusion limit for several near detector distances  $d$  and our ideal near detectors (CPT invariance assumed; 90% CL, 2 d.o.f.; two near detectors in front of straights). The dashed curves illustrate the effect of including the averaging over the decay straight, whereas the solid curves are without this averaging. The fiducial detector masses are fixed to 200 kg. Note that there is no systematics included in this figure.

than the active volume size [64]. Our “ideal” test detectors therefore have 200 kg fiducial volume at very short distances. One can, for longer baselines, up-scale the detector mass as

$$m_{\text{Det}} \simeq \frac{d \times (d + 600 \text{ m})}{50 \text{ m} \times 650 \text{ m}} 0.2 \text{ t} \quad (15)$$

without strong geometric effects from the effective area of the detector (*i.e.*, one still operates in the far distance limit). However, one may choose a different technology for these larger detectors.

For our simulation, we use the GLOBES software [68, 69]. We define the exclusion limit as a function of  $\sin^2 2\theta$  and  $\Delta m^2$  as the excluded region obtained in a  $\chi^2$  analysis assuming a vanishing true value of  $\theta$  (*i.e.* no oscillations). In Fig. 2, we show this exclusion limit for several near detector distances including the effects of averaging over the decay straight (dashed curves) and without averaging (solid curves). This figure is based on our “ideal” detectors without taking into account systematics yet. Obviously, the optimal detector locations depend on the region of sensitivity of  $\Delta m^2$  which is of interest: the smaller  $\Delta m^2$ , the longer the baseline. For instance, for  $\Delta m^2 \simeq 1 \text{ eV}^2$ , best sensitivity is obtained for  $d \simeq 20 \text{ km}$ , whereas for  $\Delta m^2 \simeq 100 \text{ eV}^2$ , a distance of the order  $d = 100 \text{ m}$  is optimal. For

short distances  $d$  up to a few hundred meters, there is clearly an effect of the averaging over the decay straight. However, note that because of the  $1/L^2$  weighting in Eq. (12), the effect becomes negligible for  $d \gtrsim 1$  km. Compared to a classical beam dump experiment, one cannot get arbitrarily close to the source without losing information. In the next section, we will discuss the requirements for systematics.

We have also tested a low energy neutrino factory for this measurement, with similar success. However, in the absence of official numbers for the storage ring geometry and systematics, we will not discuss it in greater detail. In addition, note that the absolute performance is not *a priori* better than for a higher energy neutrino factory. For instance, assume that the distance  $d$  is fixed for geometry reasons. Then the oscillation effect is, to a first approximation, proportional to  $1/E^2$  (with  $E$  the peak energy of the spectrum), but the statistics roughly increases as  $E^3$  ( $E^2$  from the beam collimation and  $E$  from the cross sections), which means that the net effect is proportional to  $E_\mu$ . We observed this behavior in our simulation.

### 3 Requirements for systematics

As far as systematics is concerned, it is well known from reactor experiments, such as Double Chooz [70] and Daya Bay [71], that electron neutrino disappearance is most affected by the signal normalization uncertainty (see, *e.g.*, Refs. [72, 73]). We expect the same for our measurement. However, compared to reactor experiments, our signal normalization error does not mainly come from the knowledge on the flux, which we may know to the level of 0.1% using various mean monitoring devices [64], but from the knowledge of the cross sections. Because our neutrino energies span the cross section regimes from quasi-elastic scattering, over resonant pion production, to deep inelastic scattering, it is not *a priori* simple to estimate the accuracy of the cross sections knowledge at the time of the measurement. For reactor experiments, on the other hand, the inverse beta decay cross sections are well known. Note that Ref. [29] also uses this well-understood detection reaction for a low-gamma beta beam, whereas we will use a completely orthogonal strategy.

Let us first of all illustrate what the main requirements for systematics are. As indicated above, we have tested in Fig. 3 the impact of a signal normalization error and an additional tilt error (tilting the shape of the spectrum). Although the errors are assumed to be rather optimistic (2.5%), there is a significant impact on the sensitivities at all baselines, as we expected. Off the oscillation maxima, as visible in the right panel at large values of  $\Delta m^2$  where  $P_{ee} \simeq 0.5 \sin^2 2\theta$ , the signal normalization error  $\sigma_{\text{Norm}}$  directly limits the sensitivity to  $\sin^2 2\theta \simeq 2 \sqrt{2.3} \sigma_{\text{Norm}} \simeq 0.076$  at  $1\sigma$  (2.3 is the  $\Delta\chi^2$  corresponding to  $1\sigma$  for two degrees of freedom). The tilt error tilts the spectrum linearly, and is a first order approximation for a shape error. It is especially important where the spectral information leads to a good sensitivity, in particular, for the shorter baselines (left panel). However, note that this (linear) tilt error cannot fully take into account the uncertainties in the cross sections, because the actual deviation may be non-linear. We have also tested the impact of backgrounds, energy resolution and energy threshold. The most important of these three systematics is the background, where the sensitivity is basically limited by the product of background



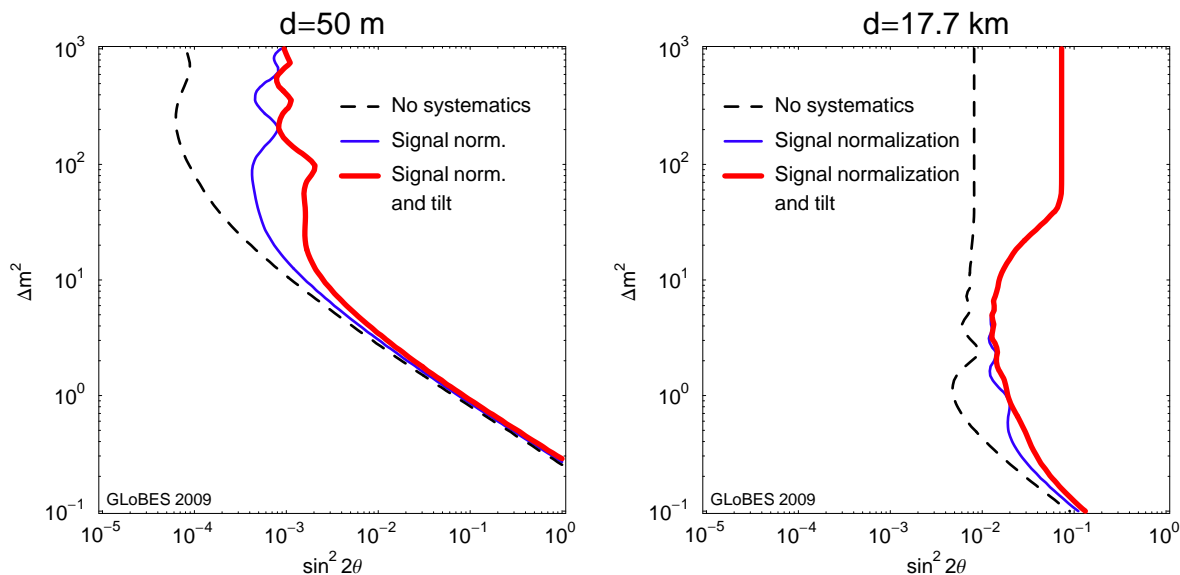


**Figure 3:** The effect of a different (hypothetical) systematical errors: A signal normalization error of 2.5% and an additional spectral tilt error of 2.5% has been applied to the exclusion limit for two different detector distances  $d$  (90% CL, 2 d.o.f.). The dashed curves refer to our ideal detectors, the solid curves include systematics. Here the fiducial mass is fixed to 200 kg, the effect of averaging over the decay straight is taken into account. Here CPT invariance is assumed.

level and background uncertainty. Even for large uncertainties of the background, such as 20%, this product limits the sensitivity to about  $0.001 \times 20\% \simeq 10^{-4}$ , which is beyond our expectations in the presence of a normalization uncertainty.

In summary, the signal normalization and shape have to be either very well known, or very well measured. The first requirement means that one needs very refined theoretical models for the cross sections, the second possibility means that one needs to measure the cross sections very well. We follow the second approach by considering a setup with two sets of detectors (*cf.*, Fig. 1):

1. Near detectors at  $d = 50$  m with  $m_{\text{Det}} = 200$  kg.
2. Far detectors at  $d = 2000$  m with  $m_{\text{Det}} = 32$  t.

The signal measured with the near detectors fixes the normalization and shape of the unoscillated signal (for small enough  $\Delta m^2$ ). The far detectors are up-scaled versions of the near detectors following Eq. (15), which means that geometric effects are almost negligible. The near detectors have optimal sensitivity at a few hundred  $\text{eV}^2$  (VSBL), whereas the far detectors have optimal sensitivity at a few  $\text{eV}^2$  (SBL). Note that longer baselines may be even better for the far detectors, but then the depth difference between storage ring and detectors may become unrealistically large. On the other hand, for distances much shorter than 2 km, one significantly loses sensitivity for small  $\Delta m^2$ .

For systematics, we adopt the most conservative point of view, *i.e.*, we assume that we hardly know anything about the cross sections, neither the normalization nor the shape, but that the cross sections are fully correlated among all detectors measuring the cross sections. Such an error is often called “shape error” and is uncorrelated among the bins. In summary, we include the following systematical errors similar to the reactor experiments in Ref. [73], and we have tested their impact (we have switched off systematical errors to test their impact):

**Shape errors** uncorrelated among bins and  $\nu\bar{\nu}$ , but fully correlated among the detectors.

These errors include cross section errors, scintillator or detector material properties, *etc.*. In addition, flux errors can be included here (the detectors only measure the product of flux and cross section for the disappearance channel). We estimate this error to be 10%. However, even a larger error does not matter if both near and far detectors are present, but only errors considerably smaller than  $10^{-3}$  improve the result significantly (which is absolutely unrealistic for this type of systematics).

**Normalization errors** uncorrelated between the near and far detectors. These relative normalization errors come from the knowledge on fiducial mass, detector normalization, and analysis cuts (uncorrelated between the detectors). They are typically small if similar detectors are used. For reactor experiments (Double Chooz [70]), this error is about 0.6%, which we use as an estimate. We have tested that there is little dependence on this error unless it can be reduced to the level of  $10^{-4}$  (then there is a small improvement), if the other systematics is present.

**Energy calibration errors** uncorrelated between the near and far detectors of the order 0.5% are used (similar to the reactor experiments). As we have tested, they are of secondary importance if all the other systematics is present.

**Backgrounds** at the level of  $10^{-3}$  from neutral current events *etc.* are assumed, known to the level of 20% (somewhat conservative estimate from a neutrino factory). If all the other errors are present, backgrounds hardly matter.

The effect of electron neutrino disappearance on the event rates of the individual bins is illustrated in Fig. 4 for the near (left) and far (right) detector for several values of  $\Delta m^2$ . For relatively small  $\Delta m^2 \sim 1 \text{ eV}^2$  (diamond curves), the near-far combination will perform similar to the reactor experiments with two detectors, where the near detector measures the shape and the far detector the oscillation effect. For  $\Delta m^2 \gg 1000 \text{ eV}^2$  (*cf.*, triangle curves for comparison), the oscillations average out in both detectors, and  $\sin^2 2\theta$  can only be constrained to the level of the shape errors (whereas  $\Delta m^2$  cannot be measured). For  $\Delta m^2 \sim 100 \text{ eV}^2$  (box curves), the oscillation effect will mainly take place in the near detector, whereas the far detector measures the shape (after averaging). For  $\Delta m^2 \sim 10 \text{ eV}^2$  (star curves), the situation is most complicated: there are oscillation effects in both detectors, which can lead to intricate parameter correlations.

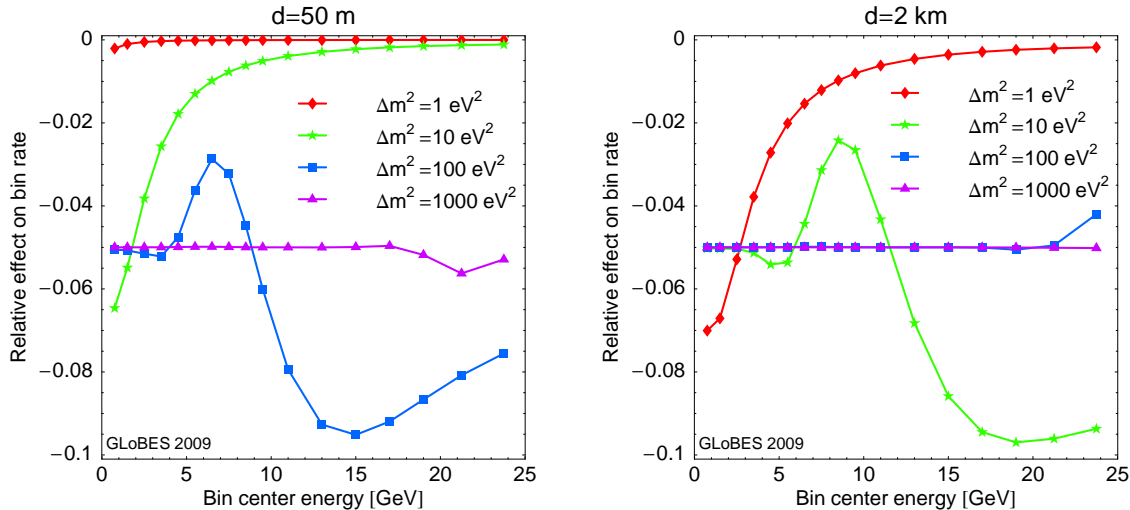


**Figure 4:** Relative effect on the binned (neutrino) event rates for several values of  $\Delta m^2$ , and  $\sin^2 2\theta = 0.1$ , in the near (left) and far (right) detectors. For each energy bin we plotted  $(R - R_0)/R_0$  where  $R$  and  $R_0$  are the expected rates with and without oscillations.

## 4 Results for CPT invariance

All results presented in this section are based on our two-baseline setup without refined systematics treatment, assuming CPT invariance, *i.e.*, the equal electron neutrino and antineutrino survival probabilities in Eq. (1).

Fig. 5 shows the performance of our near-far model (thick curve), where the effect of using only one set of detectors (near or far) is shown separately as thin curves. If only one set of detectors is used, the result will be limited by the 10% shape errors, *i.e.*, it depends on the assumptions used. However, if the two sets of detectors are used, the impact of systematics cancels and the result is very robust with respect to the assumptions. From the above discussion, it should be clear that the results in this case do not depend very much on the actual numbers for the systematical errors. Nevertheless there is a considerable deviation from the no-systematics case (dashed curve). The improvement towards this hypothetical sensitivity requires a very good understanding of the cross sections at the level of the  $\sin^2 2\theta$  sensitivity. We have also checked that the performance cannot even be significantly improved with considerably larger detectors, because of the systematics limitation (even without the geometric effect of the beam included).

Figure 5 shows that the sensitivity of a neutrino factory experiment to (V)SBL  $\nu_e$  disappearance represents a dramatic improvement with respect to the sensitivity of reactor experiments, which is at the level of  $\sin^2 2\theta \sim 10^{-1}$  at large values of  $\Delta m^2$  (*cf.*, thin gray/cyan curve). Moreover, the neutrino factory measurement with the near-far detector setup discussed in Section 3 is model-independent, whereas reactor measurements of  $P_{e\bar{e}}$  depend on the calculated flux of  $\bar{\nu}_e$ 's produced in a reactor. Reactor neutrino experiments cannot take

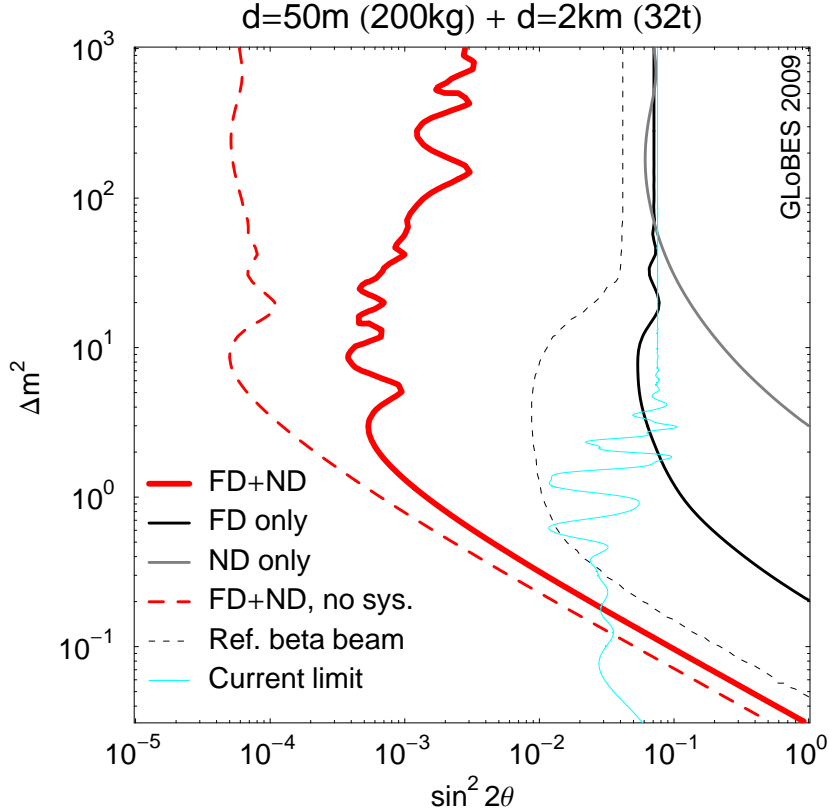


**Figure 5:** Exclusion limit in the  $\sin^2 2\theta$ - $\Delta m^2$  plane for our default configuration including systematics (thick solid curve, 90% CL, 2 d.o.f.). The thick dashed curve refers to our ideal detectors (no systematics), with near (ND) and far (FD) detectors combined. The thin solid curves illustrate the results for the near (50 m) and far (2 km) detectors if operated separately, but with full systematics. The effects of averaging over the decay straightens are taken into account. The thin dashed curve corresponds to the default beta beam setup from Ref. [29] for comparison. The thin gray/cyan curve is the current limit from Bugey [74] + Chooz [75] (taken from Ref. [16]).

advantage of the near-far detector approach to get a model-independent result for (V)SBL  $\nu_e$  disappearance, because for a typical reactor neutrino energy of 1 MeV the oscillation length corresponding to  $\Delta m^2 \approx 10^2 \text{ eV}^2$  is of the order of 1 cm.

It is interesting to note that the near-far detector setup that we have chosen is sensitive to  $\nu_e$  disappearance with small mixing ( $\sin^2 2\theta \gtrsim 2 \times 10^{-3}$ ) for values of  $\Delta m^2$  as large as  $10^3 \text{ eV}^2$ . The condition for the observation of a spectral distortion caused by neutrino oscillations is that the uncertainty of the phase of the oscillations due to the energy resolution in Eq. (10) is smaller than about  $\pi/2$ . One can easily find that this happens for neutrino energies

$$E \gtrsim \left[ \frac{\varepsilon \Delta m^2 L_{\text{eff}}}{2\pi E_0^{1/2}} \right]^{2/3}, \quad (16)$$

where we have considered the effective baseline in Eq. (14). Since for the near detector  $L_{\text{eff}} \simeq 180 \text{ m}$ , if  $\Delta m^2 = 10^3 \text{ eV}^2$  the condition (16) is satisfied for  $E \gtrsim 18 \text{ GeV}$ . Since

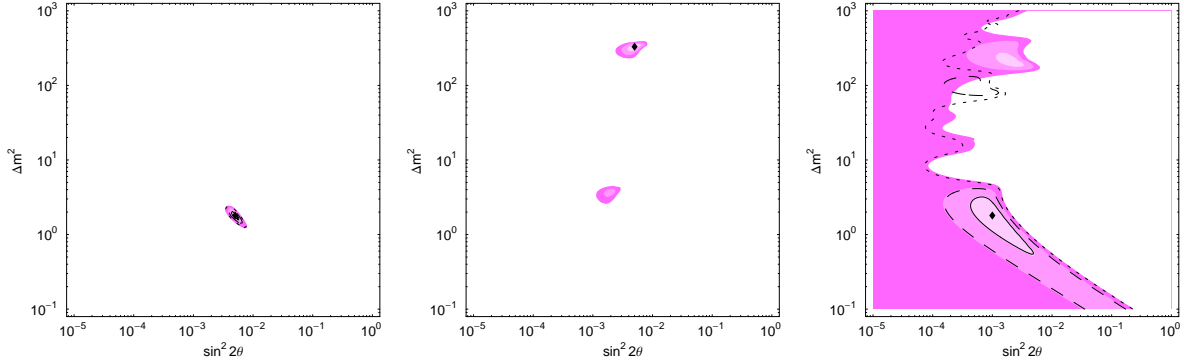


**Figure 6:** Fits in the  $\sin^2 2\theta$ - $\Delta m^2$  plane for three chosen test-points marked by the diamonds ( $1\sigma$ ,  $2\sigma$ ,  $3\sigma$ , 2 d.o.f.). Here CPT invariance is assumed. Near (50 m) and far (2 km) detectors are used with our systematics model, the effects of averaging over the decay straights are taken into account. The unshaded contours show the result without averaging effects over the straights. They are too small to be visible in the middle panel.

for the assumed  $E_\mu = 25$  GeV the neutrino energy spectrum extends up to 25 GeV, as shown by the curve in Fig.1 of Ref. [67] with off-axis angle  $\theta = 0^\circ$ , the oscillations are not completely averaged out in the highest-energy bins. This is illustrated in the left panel of Fig. 4, in which the line corresponding to  $\Delta m^2 = 10^3$  eV has the constant averaged value  $0.5 \sin^2 2\theta - 1 = -0.05$  (for the assumed  $\sin^2 2\theta = 0.1$ ) only for  $E \lesssim 10$  GeV. Other curves illustrate the distortion of the event rate spectrum for smaller values of  $\Delta m^2$ . One can see that the lower limit of the sensitivity to  $\Delta m^2$  of the near detector is about  $1 \text{ eV}^2$ , which instead produces a strong spectral distortion in the far detector (right panel of Fig. 4).

We also show in Fig. 5 a comparison with the default setup in Ref. [29] (thin dashed curve). This setup uses a low-gamma ( $\gamma \simeq 30$ ) beta beam using inverse beta decay as detection interaction, which means that it is not surprising that our result is about an order of magnitude better. Compared to Ref. [29], which uses only one detector and therefore runs in the systematics limitation in the larger  $\Delta m^2$  range, we also have very good sensitivity for large  $\Delta m^2$ . While both approaches rely on near detectors receiving neutrinos from a storage ring, they are conceptually very different: Ref. [29] uses the fact that the inverse beta decay reaction is well known to control systematics, whereas we control the shape error with two sets of detectors in the fashion of the new generation of reactor experiments.

It is interesting to examine not only the sensitivity of our experimental setup to (V)SBL  $\nu_e$  disappearance, which corresponds to a negative result producing an exclusion curve as that in Fig. 5, but also what could be the results if a signal is observed, *i.e.*,  $\nu_e$  and  $\bar{\nu}_e$  disappear.

In Fig. 6, we show three qualitatively different possible results for the test values of the neutrino oscillation parameters marked by the diamonds. In the left panel, no degenerate solutions are present, and the parameters can be very well measured. There is hardly an effect of the averaging over the decay straights, as one can read off from the differences between the shaded and unshaded contours, because the far detectors dominate the sensitivity

and oscillations have not yet developed at the near detectors. In the middle panel, we still have an excellent measurement dominated by the near detectors. In this case, however, the averaging effects over the straights are very important, and the contours without averaging are hardly visible. In particular, a degenerate solution appears at a smaller  $\Delta m^2$ . In the right panel, we show an even more extreme case, where only at the  $2\sigma$  confidence level  $\sin^2 2\theta = 0$  can be excluded.

## 5 CPT violation

In this section we discuss the potentiality of the experimental setup described in Fig. 1, with two pairs of near-far detectors, to reveal a violation of CPT symmetry, considering the different electron neutrino and antineutrino survival probabilities in Eqs. (2) and (3) as functions of the CPT asymmetries in Eq. (5).

Since there are four independent parameters, given by Eqs. (6)–(9), for simplicity we consider three test points inspired by Refs. [16–18]:

$$\text{T1 :} \quad \sin^2 2\theta = 0.05, \quad \Delta m^2 = 1.8 \text{ eV}^2, \quad (17)$$

$$\text{T2 :} \quad \sin^2 2\theta = 0.1, \quad \Delta m^2 = 20 \text{ eV}^2, \quad (18)$$

$$\text{T3 :} \quad \sin^2 2\theta = 0.1, \quad \Delta m^2 = 330 \text{ eV}^2, \quad (19)$$

and  $a_{\text{CPT}} = m_{\text{CPT}} = 0$ . We fit the corresponding simulated data allowing for non-zero values of  $a_{\text{CPT}}$  and  $m_{\text{CPT}}$  in order to explore the sensitivity to the measurement of these parameters.

The test point T1 is motivated by the best-fit of the data of the Bugey SBL reactor experiment [74], which is compatible with the data of the Chooz reactor experiment [75] and the neutrino oscillation explanation of the Gallium anomaly [16]. The test points T2 and T3 are motivated by a possible explanation the MiniBooNE low-energy anomaly through VSBL  $\nu_e$  disappearance which is compatible with the neutrino oscillation explanation of the Gallium anomaly [17, 18]. Even if values of  $\Delta m^2$  larger than about  $1 \text{ eV}^2$  are incompatible with the existing standard cosmological bound on the sum of neutrino masses [9, 76], we think that it is wise to test such bound in laboratory experiments. A violation of the bound may lead to a discovery of fundamental new physics related to non-standard cosmological effects.

The best-fit regions for the three test points are shown in Fig. 7. The dashed curves represent the results without taking into account the averaging over the decay straights. The test-point T1 (upper row), with a relatively small  $\Delta m^2$ , is dominated by the far detectors, whereas in the near detectors (almost) no oscillations are present. Therefore, the cross sections can be directly reconstructed from the near detectors, and the fits are very clean. The effects of averaging over the straights are small because the signal sits in the far detectors, which sees a point source. The oscillation parameters can be measured at the level of 2% ( $1\sigma$ ), and the CPT invariance can be constrained at the same level.

The test-point T3 (lower row of Fig. 7), is dominated by the short baseline, which means that the averaging effects over the straights are very important. The longer baseline measures the product of cross sections and  $1 - 0.5 \sin^2 2\theta$ , which means that  $\Delta m^2$  can, before the

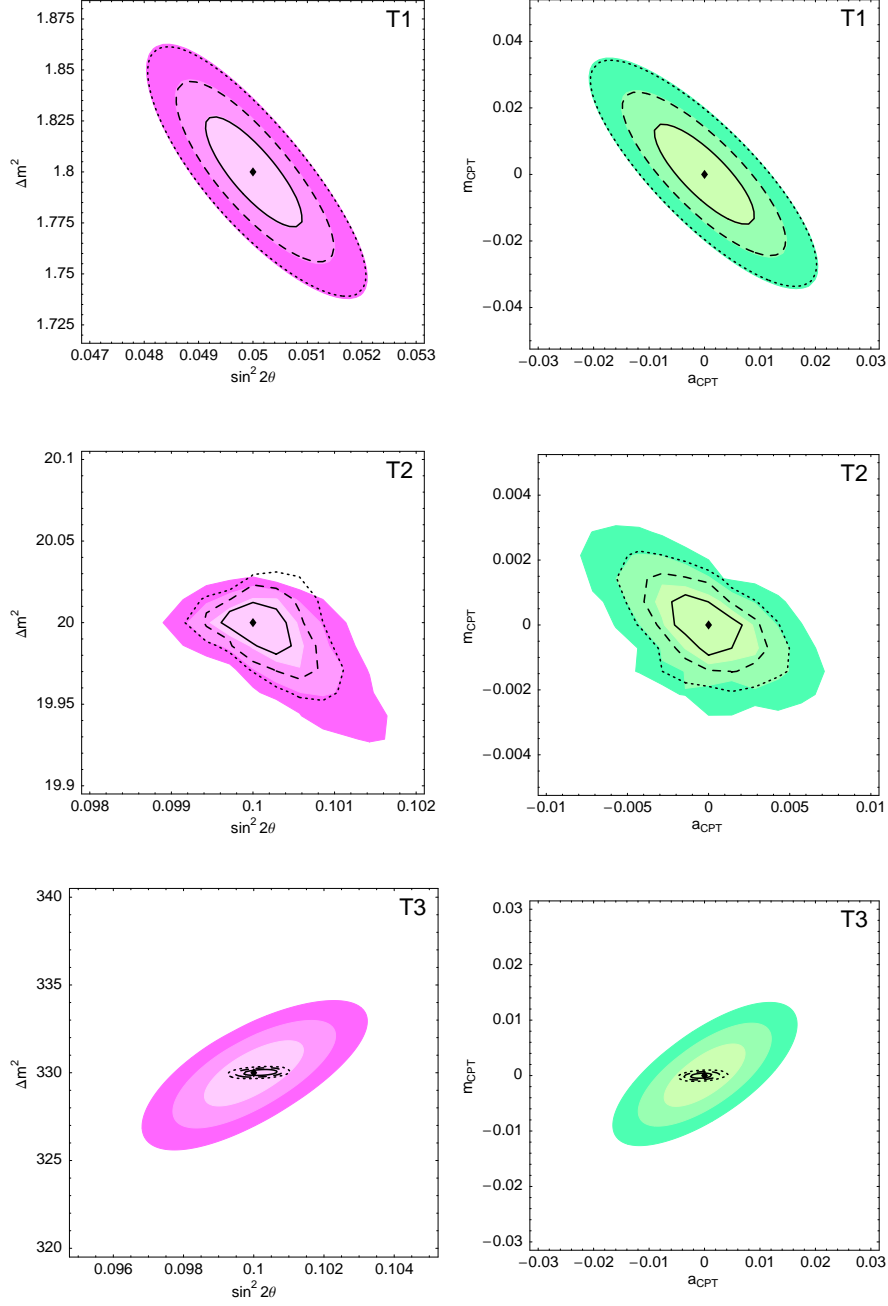


**Figure 7:** Best-fit regions in the  $\Delta m^2$ - $\sin^2 2\theta$  and  $a_{\text{CPT}}$ - $m_{\text{CPT}}$  planes for the test points defined in the main text ( $1\sigma$ ,  $2\sigma$ ,  $3\sigma$ , 2 d.o.f.). Note that different baselines were chosen for the test points. The dashed curves represent the results without taking into account the averaging over the decay straight.

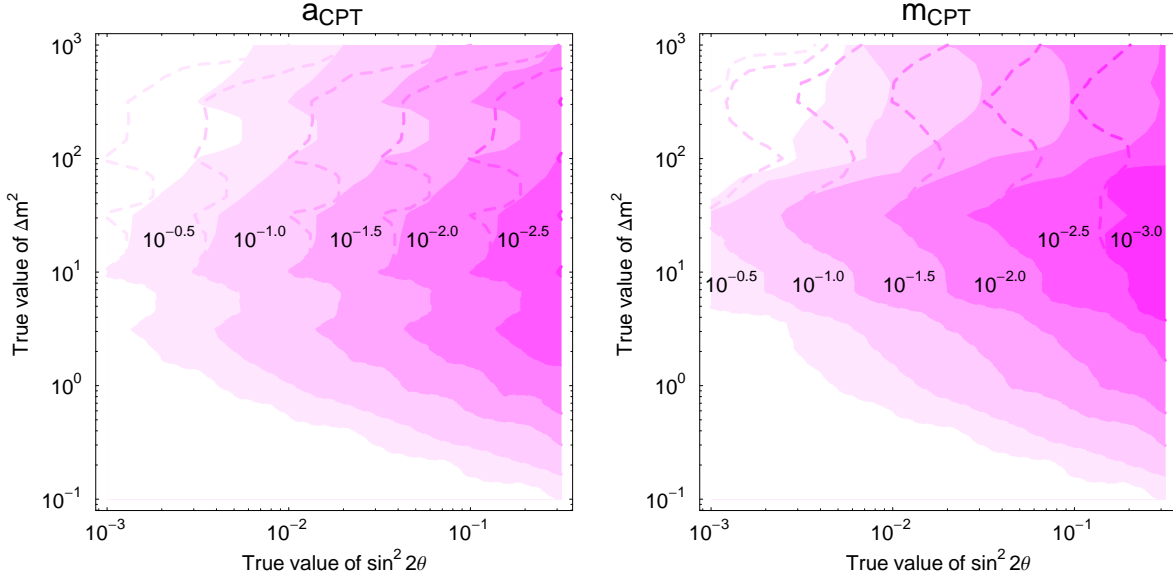


**Figure 8:** Discovery reach for CPT violation from  $a_{\text{CPT}}$  (left panel) or  $m_{\text{CPT}}$  (right panel) as a function of the true  $\sin^2 2\theta$  and true  $\Delta m^2$ . The different contours indicate for how small (true) values of  $a_{\text{CPT}} > 0$  (left) or  $m_{\text{CPT}} > 0$  (right) CPT violation will be discovered at the  $3\sigma$  confidence level, as labeled at the contours. The dashed curves show the result if the averaging over the decay straight is not taken into account.

averaging over the straight (dashed curves), be very well measured compared to the mixing angle since it remains as a net effect between the two detectors. Only after the averaging effects, both oscillation parameters can be measured at the level of 1% ( $1\sigma$ ), and the CPT invariance can be constrained at a similar level.

The test-point T2 (middle row of Fig. 7) shows a complicated case with an intricate interplay between systematics and oscillation parameter correlations. Since there is an oscillation effect in both baselines, this case does not correspond to a classical near-far detector combination. The a priori excellent precisions for the oscillation parameters are spoiled by some complicated correlations. Nevertheless, percent level precisions are possible.

Instead of constraining CPT invariance, we can also discuss the discovery reach for CPT violation. In this case, we assume that nature has implemented a small (positive)  $a_{\text{CPT}}$  or  $m_{\text{CPT}}$ , and we fit the simulated data with the fixed parameters  $a_{\text{CPT}} = m_{\text{CPT}} = 0$  (corresponding to CPT invariance), while we marginalize over the oscillation parameters  $\sin^2 2\theta$  and  $\Delta m^2$ . We show in Fig. 8 the discovery reach for CPT violation from  $a_{\text{CPT}}$  (left panel) or  $m_{\text{CPT}}$  (right panel) as a function of the true  $\sin^2 2\theta$  and true  $\Delta m^2$ . The different contours indicate for how small (true) values of  $a_{\text{CPT}} > 0$  (left) or  $m_{\text{CPT}} > 0$  (right) CPT violation will be discovered at the  $3\sigma$  confidence level, as labeled at the contours. The dashed curves show the result if the averaging over the decay straight is not taken into account.

From Fig. 8, CPT violation may be discovered even if it is as small as  $10^{-3}$ , provided that  $\sin^2 2\theta$  is large enough. However, even for very small  $\sin^2 2\theta$ , a CPT violation of order unity is testable with our setup. Note that for larger  $\Delta m^2$  and especially for  $m_{\text{CPT}}$ , the



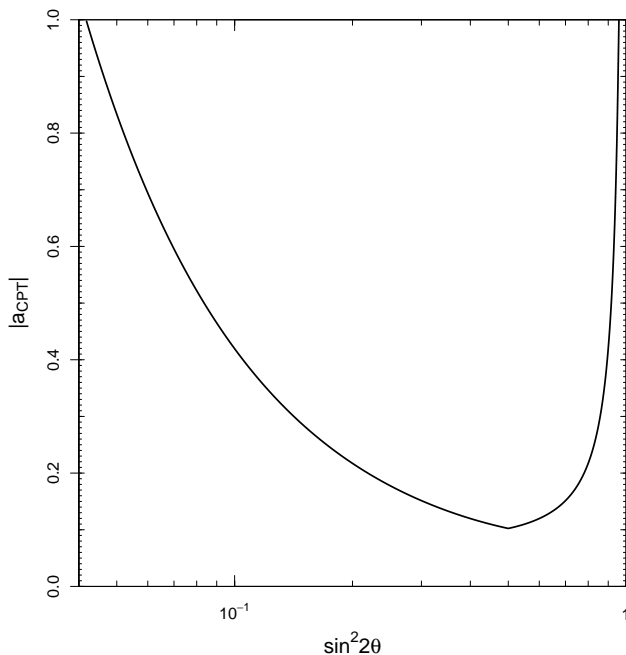


**Figure 9:** Lower limit for  $|a_{\text{CPT}}|$  obtained from Eq. (21) with  $A_{ee}^{\text{CPT}} < -0.08$ , which is the 95% C.L. limit found in Ref. [18].

averaging over the decay straights strongly reduces the performance (by about one order of magnitude).

In Ref. [18], a difference of  $A_{ee}^{\text{CPT}} \equiv P_{ee} - P_{\bar{e}\bar{e}} = -0.17_{-0.07}^{+0.09}$  at 90% C.L. was identified as the asymmetry between the electron neutrino and anti-neutrino VSBL disappearance probabilities which can explain the Gallium radioactive source experiments anomaly [14] and the MiniBooNE low-energy anomaly [13] without conflicting with the absence of  $\bar{\nu}_e$  disappearance in reactor neutrino experiments (see Ref. [77]). It is interesting to investigate if such CPT violation can be measured in a neutrino factory experiment with the near-far pairs of detectors that we have considered so far.

Since in Ref. [18]  $\Delta m^2$  was considered to be large, in the range

$$20 \text{ eV}^2 \lesssim \Delta m^2 \lesssim 330 \text{ eV}^2, \quad (20)$$

the neutrino and antineutrino survival probabilities were assumed to be averaged, leading to  $A_{ee}^{\text{CPT}} = 0.5 (\sin^2 2\theta_\nu - \sin^2 2\theta_{\bar{\nu}})$ . In this case, the asymmetry  $a_{\text{CPT}}$  is given by

$$a_{\text{CPT}} = \frac{1}{4\theta} \arcsin \left( \frac{-2A_{ee}^{\text{CPT}}}{\sin 4\theta} \right). \quad (21)$$

Since  $|a_{\text{CPT}}| \leq 1$ , the mixing angle has a lower limit which depends on the value of  $A_{ee}^{\text{CPT}}$ . Moreover, since  $|\sin 4\theta| \leq 1$  and  $\theta \leq \pi/2$ , also  $|a_{\text{CPT}}|$  has a lower limit, which is plotted in Fig. 9 for  $A_{ee}^{\text{CPT}} < -0.08$ , which is the 95% C.L. limit found in Ref. [18]. One can see that the bound on  $A_{ee}^{\text{CPT}}$  implies that  $\sin^2 2\theta \gtrsim 4 \times 10^{-2}$  and  $|a_{\text{CPT}}| \gtrsim 0.10$ . Confronting these values with the left panel in Fig. 8, and taking into account that we consider the large values

of  $\Delta m^2$  in the range (20), it is clear that the CPT violation required by  $A_{ee}^{\text{CPT}} \lesssim -0.08$  will be easily discovered in a neutrino factory experiment with the near-far pairs of detectors that we have considered.

## 6 Summary and conclusions

In this work we have discussed the potentiality of testing Short-BaseLine (SBL, with  $10^{-1} \lesssim \Delta m_{\text{SBL}}^2 \lesssim 10 \text{ eV}^2$ ) and Very-Short-BaseLine (VSBL, with  $10 \lesssim \Delta m_{\text{VSBL}}^2 \lesssim 10^3 \text{ eV}^2$ ) electron neutrino disappearance in a neutrino factory experiment, based on the current setup of the International Design Study for the Neutrino Factory (IDS-NF) [63]. Since this setup uses both muon and anti-muon decays, a possible difference between the neutrino and antineutrino disappearance can be studied, which could constitute a revolutionary discovery of CPT violation.

We showed that for these purposes the ideal configuration would be the two pairs of near-far detectors (shown in Fig. 1) in a similar fashion to reactor experiments with near and far detectors (Double Chooz [70], Daya Bay [71], *etc.*) to cancel systematics. The near detectors are chosen to be at a distance of about 50 m from the muon storage ring, in order to be sensitive to oscillations due to a  $\Delta m^2$  as large as about  $10^3 \text{ eV}^2$ . For the far detectors an appropriate distance from the muon storage ring is about 2 km, which gives a good sensitivity to oscillations generated by a  $\Delta m^2$  as small as about  $10^{-1} \text{ eV}^2$ . In this way, it is possible to explore (V)SBL  $\nu_e$  and  $\bar{\nu}_e$  disappearance with effective oscillation amplitude  $\sin^2 2\theta$  as small as about  $10^{-3}$  for  $\Delta m^2 \gtrsim 1 \text{ eV}^2$  (see Fig. 5) taking advantage of the comparison of the event rates measured in the near and far detectors, which reduces dramatically the systematic uncertainties due to insufficient knowledge of the cross sections (see the discussion in Section 3).

We have also shown, in Section 5, that the chosen detector setup provides a good sensitivity to the measurement of a difference of the rates of  $\nu_e$  and  $\bar{\nu}_e$  disappearance which would be a signal of CPT violation. For instance, our setup is sensitive to an asymmetry between the neutrino and antineutrino mass squared differences at the level of up to  $10^{-3}$ , depending on the value of the mixing angle. Let us emphasize that a discovery of CPT violation would represent a revolution in our knowledge of fundamental physics, because the CPT symmetry is a fundamental symmetry of local relativistic Quantum Field Theory. Therefore, pursuing this line of investigation is of fundamental importance.

## Acknowledgments

We would like to thank Sanjib Agarwalla for providing the beta beam reference curve in Fig. 5, and Patrick Huber for useful discussions.

This work was supported by the European Union under the European Commission Framework Programme 07 Design Study EUROnu, Project 212372. W. Winter also would like to acknowledge support from the Emmy Noether program of Deutsche Forschungsgemeinschaft.

C. Giunti would like to thank the Department of Theoretical Physics of the University of Torino for hospitality and support.

## References

- [1] S.M. Bilenky, C. Giunti and W. Grimus, *Prog. Part. Nucl. Phys.* 43 (1999) 1, [arXiv:hep-ph/9812360](#).
- [2] M. Gonzalez-Garcia and Y. Nir, *Rev. Mod. Phys.* 75 (2003) 345, [arXiv:hep-ph/0202058](#).
- [3] C. Giunti and M. Laveder, (2003), [arXiv:hep-ph/0310238](#), In “Developments in Quantum Physics – 2004”, p. 197-254, edited by F. Columbus and V. Krasnoholovets, Nova Science Publishers, Inc.
- [4] M. Maltoni et al., *New J. Phys.* 6 (2004) 122, [arXiv:hep-ph/0405172](#).
- [5] G.L. Fogli et al., *Prog. Part. Nucl. Phys.* 57 (2006) 742, [arXiv:hep-ph/0506083](#).
- [6] A. Strumia and F. Vissani, (2006), [arXiv:hep-ph/0606054](#).
- [7] C. Giunti and C.W. Kim, *Fundamentals of Neutrino Physics and Astrophysics* (Oxford University Press, 2007).
- [8] M.C. Gonzalez-Garcia and M. Maltoni, *Phys. Rept.* 460 (2008) 1, [arXiv:0704.1800](#).
- [9] G.L. Fogli et al., *Phys. Rev. D* 78 (2008) 033010, [arXiv:0805.2517](#).
- [10] T. Schwetz, M. Tortola and J.W.F. Valle, *New J. Phys.* 10 (2008) 113011, [arXiv:0808.2016](#).
- [11] LSND, A. Aguilar et al., *Phys. Rev. D* 64 (2001) 112007, [arXiv:hep-ex/0104049](#).
- [12] KARMEN, B. Armbruster et al., *Phys. Rev. D* 65 (2002) 112001, [arXiv:hep-ex/0203021](#).
- [13] MiniBooNE, A.A. Aguilar-Arevalo, *Phys. Rev. Lett.* 102 (2009) 101802, [arXiv:0812.2243](#).
- [14] SAGE, J.N. Abdurashitov et al., *Phys. Rev. C* 80 (1990) 015807, [arXiv:0901.2200](#).
- [15] C. Giunti and M. Laveder, *Mod. Phys. Lett. A* 22 (2007) 2499, [arXiv:hep-ph/0610352](#).
- [16] M.A. Acero, C. Giunti and M. Laveder, *Phys. Rev. D* 78 (2008) 073009, [arXiv:0711.4222](#).
- [17] C. Giunti and M. Laveder, *Phys. Rev. D* 77 (2008) 093002, [arXiv:0707.4593](#).
- [18] C. Giunti and M. Laveder, *Phys. Rev. D* 80 (2009) 013005, [arXiv:0902.1992](#).

- [19] M. Sorel, J. Conrad and M. Shaevitz, Phys. Rev. D70 (2004) 073004, [arXiv:hep-ph/0305255](#).
- [20] G. Karagiorgi et al., (2009), [arXiv:0906.1997](#).
- [21] G. Karagiorgi et al., Phys. Rev. D75 (2007) 013011, [arXiv:hep-ph/0609177](#).
- [22] C. Grieb, J. Link and R.S. Raghavan, Phys. Rev. D75 (2007) 093006, [arXiv:hep-ph/0611178](#).
- [23] D.C. Latimer, J. Escamilla and D.J. Ernst, Phys. Rev. C75 (2007) 042501, [arXiv:hep-ex/0701004](#).
- [24] A. Donini et al., JHEP 12 (2007) 013, [arXiv:0704.0388](#).
- [25] M. Maltoni and T. Schwetz, Phys. Rev. D76 (2007) 093005, [arXiv:0705.0107](#).
- [26] S. Goswami and W. Rodejohann, JHEP 10 (2007) 073, [arXiv:0706.1462](#).
- [27] A. Bandyopadhyay and S. Choubey, (2007), [arXiv:0707.2481](#).
- [28] T. Schwetz, JHEP 02 (2008) 011, [arXiv:0710.2985](#).
- [29] S.K. Agarwalla, P. Huber and J.M. Link, (2009), [arXiv:0907.3145](#).
- [30] R.L. Awasthi and S. Choubey, Phys. Rev. D76 (2007) 113002, [arXiv:0706.0399](#).
- [31] S. Choubey, JHEP 12 (2007) 014, [arXiv:0709.1937](#).
- [32] D. Boyanovsky, H.J. de Vega and N. Sanchez, Phys. Rev. D77 (2008) 043518, [arXiv:0710.5180](#).
- [33] G. Gentile, H.S. Zhao and B. Famaey, (2007), [arXiv:0712.1816](#).
- [34] G.W. Angus, (2008), [arXiv:0805.4014](#).
- [35] A. Donini and O. Yasuda, (2008), [arXiv:0806.3029](#).
- [36] O. Civitarese and M.E. Mosquera, Phys. Rev. C77 (2008) 045806, [arXiv:0711.2450](#).
- [37] A. Melchiorri et al., JCAP 0901 (2009) 036, [arXiv:0810.5133](#).
- [38] M.A. Acero and J. Lesgourgues, Phys. Rev. D79 (2009) 045026, [arXiv:0812.2249](#).
- [39] O.W. Greenberg, Found. Phys. 36 (2006) 1535, [arXiv:hep-ph/0309309](#).
- [40] O.W. Greenberg, Phys. Rev. Lett. 89 (2002) 231602, [arXiv:hep-ph/0201258](#).
- [41] G. Barenboim et al., Phys. Lett. B537 (2002) 227, [arXiv:hep-ph/0203261](#).
- [42] V.A. Kostelecky and N. Russell, (2008), [arXiv:0801.0287](#).
- [43] H. Murayama and T. Yanagida, Phys. Lett. B520 (2001) 263, [arXiv:hep-ph/0010178](#).

- [44] G. Barenboim et al., JHEP 10 (2002) 001, [arXiv:hep-ph/0108199](#).
- [45] S.M. Bilenky et al., Phys. Rev. D65 (2002) 073024, [arXiv:hep-ph/0112226](#).
- [46] G. Barenboim, L. Borissov and J. Lykken, Phys. Lett. B534 (2002) 106, [arXiv:hep-ph/0201080](#).
- [47] A. Strumia, Phys. Lett. B539 (2002) 91, [arXiv:hep-ph/0201134](#).
- [48] J.N. Bahcall, V. Barger and D. Marfatia, Phys. Lett. B534 (2002) 120, [arXiv:hep-ph/0201211](#).
- [49] H. Murayama, Phys. Lett. B597 (2004) 73, [arXiv:hep-ph/0307127](#).
- [50] V. Barger, D. Marfatia and K. Whisnant, Phys. Lett. B576 (2003) 303, [arXiv:hep-ph/0308299](#).
- [51] H. Minakata and S. Uchinami, Phys. Rev. D72 (2005) 105007, [arXiv:hep-ph/0505133](#).
- [52] M.C. Gonzalez-Garcia, M. Maltoni and T. Schwetz, Phys. Rev. D68 (2003) 053007, [arXiv:hep-ph/0306226](#).
- [53] S. Antusch and E. Fernandez-Martinez, Phys. Lett. B665 (2008) 190, [arXiv:0804.2820](#).
- [54] A.D. Dolgov, (2009), [arXiv:0903.4318](#).
- [55] MINOS, J. Evans, (2009), HEP 2009, The 2009 Europhysics Conference on High Energy Physics, 16-22 July 2009, Krakow, Poland. URL: <http://indico.ifj.edu.pl/MaKaC/contributionDisplay.py?contribId=671&sessionId=8&confI>
- [56] G. Barenboim and J.D. Lykken, (2009), [arXiv:0908.2993](#).
- [57] V.A. Kostelecky and M. Mewes, Phys. Rev. D69 (2004) 016005, [arXiv:hep-ph/0309025](#).
- [58] D. Hooper, D. Morgan and E. Winstanley, Phys. Rev. D72 (2005) 065009, [arXiv:hep-ph/0506091](#).
- [59] T. Katori, V.A. Kostelecky and R. Tayloe, Phys. Rev. D74 (2006) 105009, [arXiv:hep-ph/0606154](#).
- [60] S. Hollenberg, O. Micu and H. Pas, (2009), [arXiv:0906.5072](#).
- [61] S. Esposito and G. Salesi, (2009), [arXiv:0906.5542](#).
- [62] J.L.B. Alba et al., (2009), [arXiv:0907.1979](#).
- [63] International design study of the neutrino factory, <http://www.ids-nf.org>.
- [64] ISS Detector Working Group, T. Abe et al., (2009), [arXiv:0712.4129](#).

- [65] S. Geer, O. Mena and S. Pascoli, Phys. Rev. D75 (2007) 093001, [arXiv:hep-ph/0701258](#).
- [66] A. Bross et al., Phys. Rev. D77 (2008) 093012, [arXiv:0709.3889](#).
- [67] J. Tang and W. Winter, (2009), [arXiv:0903.3039](#).
- [68] P. Huber, M. Lindner and W. Winter, Comput. Phys. Commun. 167 (2005) 195, [arXiv:hep-ph/0407333](#).
- [69] P. Huber et al., Comput. Phys. Commun. 177 (2007) 432, [arXiv:hep-ph/0701187](#).
- [70] Double Chooz, F. Ardellier et al., (2006), [arXiv:hep-ex/0606025](#).
- [71] Daya Bay, X. Guo et al., (2007), [arXiv:hep-ex/0701029](#), Proposal to DOE.
- [72] P. Huber et al., Nucl. Phys. B665 (2003) 487, [arXiv:hep-ph/0303232](#).
- [73] P. Huber et al., JHEP 05 (2006) 072, [arXiv:hep-ph/0601266](#).
- [74] Bugey, B. Achkar et al., Nucl. Phys. B434 (1995) 503.
- [75] CHOOZ, M. Apollonio et al., Eur. Phys. J. C27 (2003) 331, [arXiv:hep-ex/0301017](#).
- [76] F. De Bernardis et al., Phys. Rev. D78 (2008) 083535, [arXiv:0809.1095](#).
- [77] C. Bemporad, G. Gratta and P. Vogel, Rev. Mod. Phys. 74 (2002) 297, [arXiv:hep-ph/0107277](#).